Chapter 14

Fixed points, and how to get them

(F. Christiansen)

Having set up the dynamical context, now we turn to the key and unavoidable piece of numerics in this subject; search for the solutions (x,T), $x \in \mathbb{R}^d$, $T \in \mathbb{R}$ of the *periodic orbit condition*

$$f^{t+T}(x) = f^t(x)\,, \qquad T > 0 \tag{14.1}$$

for a given flow or mapping.

We know from chapter 11 that cycles are the necessary ingredient for evaluation of spectra of evolution operators. In chapter 9 we have developed a qualitative theory of how these cycles are laid out topologically. This chapter is intended as a hands-on guide to extraction of periodic orbits, and should be skipped on first reading - you can return to it whenever the need for finding actual cycles arises. A serious cyclist might want to also learn about the variational methods to find cycles, chapter 25. They are particularly useful when little is understood about the topology of a flow, such as in high-dimensional periodic orbit searches.

chapter 25

fast track:
chapter 15, p. 279

A *prime* cycle p of period T_p is a single traversal of the orbit, so our task will be to find a cycle point $x \in p$ and the shortest time T_p for which (14.1) has a solution. A cycle point of a flow f^t which crosses a Poincaré section n_p times is a fixed point of the P^{n_p} iterate of the Poincaré section

sect. 4.5.2

return map P, hence we shall refer to all cycles as "fixed points" in this chapter. By cyclic invariance, stability eigenvalues and the period of the cycle are independent of the choice of the initial point, so it will suffice to solve (14.1) at a single cycle point.

If the cycle is an attracting limit cycle with a sizable basin of attraction, it can be found by integrating the flow for sufficiently long time. If the cycle is unstable, simple integration forward in time will not reveal it, and methods to be described here need to be deployed. In essence, any method for finding a cycle is based on devising a new dynamical system which possesses the same cycle, but for which this cycle is attractive. Beyond that, there is a great freedom in constructing such systems, and many different methods are used in practice.

Due to the exponential divergence of nearby trajectories in chaotic dynamical systems, fixed point searches based on direct solution of the fixed-point condition (14.1) as an initial value problem can be numerically very unstable. Methods that start with initial guesses for a number of points along the cycle, such as the multipoint shooting method described here in sect. 14.3, and the variational) methods of chapter 25, are considerably more robust and safer.

chapter 25

A prerequisite for any exhaustive cycle search is a good understanding of the topology of the flow: a preliminary step to any serious periodic orbit calculation is preparation of a list of all distinct admissible prime periodic symbol sequences, such as the list given in table 9.2. The relations between the temporal symbol sequences and the spatial layout of the topologically distinct regions of the phase space discussed in chapter 9 should enable us to guess location of a series of periodic points along a cycle. Armed with such informed guess we proceed to improve it by methods such as the Newton-Raphson iteration; we illustrate this by considering 1-dimensional and d-dimensional maps.

14.1 Where are the cycles?

Ergodic exploration of recurrences that we turn to now sometimes performs admirably well in getting us started.

Both in the example of the Rössler flow and of the Kuramoto-Sivashinsky system we sketched the attractors by running a long chaotic trajectory, and noted that the attractors are very thin, but otherwise the return maps that we plotted were disquieting – neither fig. 3.2 nor fig. 3.3 appeared to be 1-to-1 maps. In this section we show how to use such information to approximately locate cycles. In the remainder of this chapter and in chapter 25 we shall learn how to turn such guesses into highly accurate cycles.

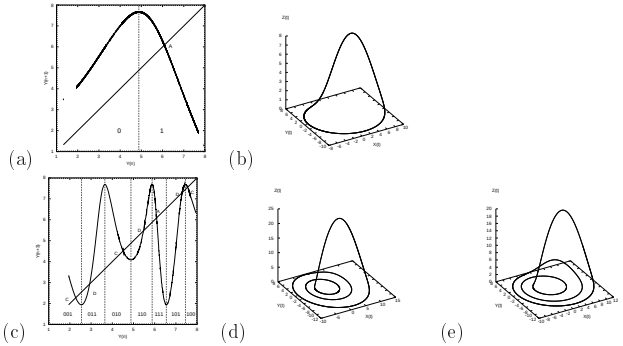

Figure 14.1: (a) $y \to P_1(y,z)$ return map for $x = 0$, $y > 0$ Poincaré section of the Rössler flow fig. 2.3. (b) The $\overline{1}$-cycle found by taking the fixed point $y_{k+n} = y_k$ together with the fixed point of the $z \to z$ return map (not shown) an initial guess $(0, y^{(0)}, z^{(0)})$ for the Newton-Raphson search. (c) $y_{k+3} = P_1^3(x_k, y_k)$, the third iterate of Poincaré return map (3.1) together with the corresponding plot for $z_{k+3} = P_2^3(x_k, y_k)$, is used to pick starting guesses for the Newton-Raphson searches for the two 3-cycles: (d) the $\overline{001}$ cycle, and (e) the $\overline{011}$ cycle. (G. Simon)

Example 14.1 Rössler attractor *(G. Simon and P. Cvitanović)*

Run a long simulation of the Rössler flow f^t, plot a Poincaré section, as in fig. 3.1, and extract the corresponding Poincaré return map P, as in fig. 3.2. Luck is with us; the fig. 14.1(a) return map $y \to P_1(y,z)$ looks much like a parabola, so we take the unimodal map symbolic dynamics, sect. 9.4, as our guess for the covering dynamics. Strictly speaking, the attractor is "fractal", but for all practical purposes the return map is 1-dimensional; your printer will need a resolution better than 10^{14} dots per inch to start resolving its structure.

Periodic points of a prime cycle p of cycle length n_p for the $x = 0$, $y > 0$ Poincaré section of the Rössler flow fig. 2.3 are fixed points $(y,z) = Pn(y,z)$ of the nth Poincaré return map.

Using the fixed point $y_{k+1} = y_k$ in fig. 14.1(a) together with the simultaneous fixed point of the $z \to P_1(y,z)$ return map (not shown) as a starting guess $(0, y^{(0)}, z^{(0)})$ for the Newton-Raphson search for the cycle p with symbolic dynamics label $\overline{1}$, we find the cycle fig. 14.1(b) with the Poincaré section point $(0, y_p, z_p)$, period T_p, expanding, marginal, contracting stability eigenvalues $(\Lambda_{p,e}, \Lambda_{p,m}, \Lambda_{p,c})$, and Lyapunov exponents $(\lambda_{p,e}, \lambda_{p,m}, \lambda_{p,c})$:

$$\begin{aligned}
\overline{1}\text{-cycle:} \quad (x,y,z) &= (0, 6.09176832, 1.2997319) \\
T_1 &= 5.88108845586 \\
(\Lambda_{1,e}, \Lambda_{1,m}, \Lambda_{1,c}) &= (-2.40395353, 1+10^{-14}, -1.29\times 10^{-14}) \\
(\lambda_{1,e}, \lambda_{1,m}, \lambda_{1,c}) &= (0.149141556, 10^{-14}, -5.44)\,. \qquad (14.2)
\end{aligned}$$

The Newton-Raphson method that we used is described in sect. 14.5.

14.7 page 276

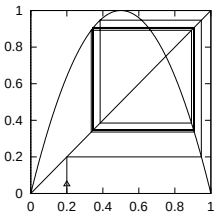

Figure 14.2: The inverse time path to the $\overline{01}$-cycle of the logistic map f(x)=4x(1-x) from an initial guess of x=0.2. At each inverse iteration we chose the 0, respectively 1 branch.

As an example of a search for longer cycles, we use $y_{k+3} = P^3(y_k, z_k)$, the third iterate of Poincaré return map (3.1) plotted in fig. 14.1(c), together with a corresponding plot for $z_{k+3} = f^3(y_k, z_k)$, to pick starting guesses for the Newton-Raphson searches for the two 3-cycles plotted in fig. 14.1(d), (e). For a listing of the short cycles of the Rössler flow, consult table 14.1.

The numerical evidence suggests (but a proof is lacking) that all cycles that comprise the strange attractor of the Rössler system are hyperbolic, each with an expanding eigenvalue $|\Lambda_e| > 1$, a contracting eigenvalue $|\Lambda_c| < 1$, and a marginal eigenvalue $|\Lambda_m| = 1$ corresponding to displacements along the direction of the flow.

For the Rössler system the contracting eigenvalues turn out to be insanely contracting, a factor of e^{-32} per one par-course of the attractor, so their numerical determination is quite difficult. Fortunately, they are irrelevant; for all practical purposes the strange attractor of the Rössler system is 1-dimensional, a very good realization of a horseshoe template.

14.2 One-dimensional mappings

14.2.1 Inverse iteration

Let us first consider a very simple method to find unstable cycles of a 1-dimensional map such as the logistic map. Unstable cycles of 1-d maps are attracting cycles of the inverse map. The inverse map is not single valued, so at each backward iteration we have a choice of branch to make. By choosing branch according to the symbolic dynamics of the cycle we are trying to find, we will automatically converge to the desired cycle. The rate of convergence is given by the stability of the cycle, i.e. the convergence is exponentially fast. Fig. 14.2 shows such path to the $\overline{01}$-cycle of the logistic map.

The method of inverse iteration is fine for finding cycles for 1-d maps and some 2-d systems such as the repeller of exercise 14.11. It is not particularly fast, especially if the inverse map is not known analytically. However, it completely fails for higher dimensional systems where we have both stable and unstable directions. Inverse iteration will exchange these, but we will

14.11 page 278

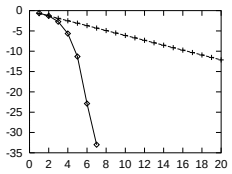

Figure 14.3: Convergence of Newton's method ($\diamondsuit$) vs. inverse iteration ($+$). The error after n iterations searching for the $\overline{01}$-cycle of the logistic map $f(x) = 4x(1-x)$ with an initial starting guess of $x_1 = 0.2, x_2 = 0.8$. y-axis is $\log_{10}$ of the error. The difference between the exponential convergence of the inverse iteration method and the super-exponential convergence of Newton's method is dramatic.

still be left with both stable and unstable directions. The best strategy is to directly attack the problem of finding solutions of $f^T(x) = x$.

14.2.2 Newton's method

Newton's method for determining a zero x^* of a function $F(x)$ of one variable is based on a linearization around a starting guess x_0:

$$F(x) \approx F(x_0) + F'(x_0)(x - x_0). \tag{14.3}$$

An approximate solution x_1 of $F(x) = 0$ is

$$x_1 = x_0 - F(x_0)/F'(x_0). \tag{14.4}$$

The approximate solution can then be used as a new starting guess in an iterative process. A fixed point of a map f is a solution to $F(x) = x - f(x) = 0$. We determine x by iterating

$$\begin{aligned} x_m &= g(x_{m-1}) = x_{m-1} - F(x_{m-1})/F'(x_{m-1}) \\ &= x_{m-1} - \frac{1}{1 - f'(x_{m-1})}(x_{m-1} - f(x_{m-1}))\,. \end{aligned} \tag{14.5}$$

Provided that the fixed point is not marginally stable, $f'(x) \neq 1$ at the fixed point x, a fixed point of f is a super-stable fixed point of the Newton-Raphson map g, $g'(x) = 0$, and with a sufficiently good initial guess, the Newton-Raphson iteration will converge super-exponentially fast.

To illustrate the efficiency of the Newton's method we compare it to the inverse iteration method in fig. 14.3. Newton's method wins hands down: the number of significant digits of the accuracy of x estimate doubles with each iteration.

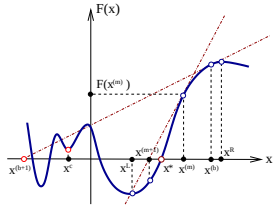

Figure 14.4: Newton method: bad initial guess $x^{(b)}$ leads to the Newton estimate $x^{(b+1)}$ far away from the desired zero of $F(x)$. Sequence $\cdots$, $x^{(m)}$, $x^{(m+1)}, \cdots$, starting with a good guess converges super-exponentially to x^*. The method diverges if it iterates into the basin of attraction of a local minimum x^c.

In order to avoid jumping too far from the desired x^* (see fig. 14.4), one often initiates the search by the *damped Newton method*,

$$\Delta x_m = x_{m+1} - x_m = -\frac{F(x_m)}{F'(x_m)}\,\Delta\tau\,, \qquad 0 < \Delta\tau \leq 1\,,$$

takes small $\Delta\tau$ steps at the beginning, reinstating to the full $\Delta\tau = 1$ jumps only when sufficiently close to the desired x^*.

14.3 Multipoint shooting method

Periodic orbits of length n are fixed points of f^n so in principle we could use the simple Newton's method described above to find them. However, this is not an optimal strategy. f^n will be a highly oscillating function with perhaps as many as 2^n or more closely spaced fixed points, and finding a specific periodic point, for example one with a given symbolic sequence, requires a *very* good starting guess. For binary symbolic dynamics we must expect to improve the accuracy of our initial guesses by at least a factor of 2^n to find orbits of length n. A better alternative is the *multipoint shooting method*. While it might very hard to give a precise initial point guess for a long periodic orbit, if our guesses are informed by a good phase-space partition, a rough guess for each point along the desired trajectory might suffice, as for the individual short trajectory segments the errors have no time to explode exponentially.

A cycle of length n is a zero of the n-dimensional vector function F:

$$F(x) = F\begin{pmatrix} x_1 \\ x_2 \\ \cdot \\ x_n \end{pmatrix} = \begin{pmatrix} x_1 - f(x_n) \\ x_2 - f(x_1) \\ \cdots \\ x_n - f(x_{n-1}) \end{pmatrix}.$$

The relations between the temporal symbol sequences and the spatial layout of the topologically distinct regions of the phase space discussed in chapter 9

enable us to guess location of a series of periodic points along a cycle. Armed with such informed initial guesses we can initiate a Newton-Raphson iteration. The iteration in the Newton's method now takes the form of

$$\frac{d}{dx}F(x)(x'-x) = -F(x), \tag{14.6}$$

where $\frac{d}{dx}F(x)$ is an $[n \times n]$ matrix:

$$\frac{d}{dx}F(x) = \begin{pmatrix} 1 & & & & -f'(x_n) \\ -f'(x_1) & 1 & & & \\ & \cdots & 1 & & \\ & & \cdots & 1 & \\ & & & -f'(x_{n-1}) & 1 \end{pmatrix}. \tag{14.7}$$

This matrix can easily be inverted numerically by first eliminating the elements below the diagonal. This creates non-zero elements in the nth column. We eliminate these and are done. Let us take it step by step for a period 3 cycle. Initially the setup for the Newton step looks like this:

$$\begin{pmatrix} 1 & 0 & -f'(x_3) \\ -f'(x_1) & 1 & 0 \\ 0 & -f'(x_2) & 1 \end{pmatrix} \begin{pmatrix} \delta_1 \\ \delta_2 \\ \delta_3 \end{pmatrix} = \begin{pmatrix} -F_1 \\ -F_2 \\ -F_3 \end{pmatrix}, \tag{14.8}$$

where $\delta_i = x'_i - x_i$ is the correction of our guess for a solution and where $F_i = x_i - f(x_{i-1})$. First we eliminate the below diagonal elements by adding $f'(x_1)$ times the first row to the second row, then adding $f'(x_2)$ times the second row to the third row. We then have

$$\begin{pmatrix} 1 & 0 & -f'(x_3) \\ 0 & 1 & -f'(x_1)f'(x_3) \\ 0 & 0 & 1 - f'(x_2)f'(x_1)f'(x_3) \end{pmatrix} \begin{pmatrix} \delta_1 \\ \delta_2 \\ \delta_3 \end{pmatrix} = \begin{pmatrix} -F_1 \\ -F_2 - f'(x_1)F_1 \\ -F_3 - f'(x_2)F_2 - f'(x_2)f'(x_1)F_1 \end{pmatrix}. \tag{14.9}$$

The next step is to invert the last element in the diagonal, i.e. divide the third row by $1 - f'(x_2)f'(x_1)f'(x_3)$. It is clear that if this element is zero at the periodic orbit this step might lead to problems. In many cases this will just mean a slower convergence, but it might throw the Newton iteration completely off. We note that $f'(x_2)f'(x_1)f'(x_3)$ is the stability of the cycle

(when the Newton iteration has converged) and that this therefore is not a good method to find marginally stable cycles. We now have

$$\begin{pmatrix} 1 & 0 & -f'(x_3) \\ 0 & 1 & -f'(x_1)f'(x_3) \\ 0 & 0 & 1 \end{pmatrix} \begin{pmatrix} \delta_1 \\ \delta_2 \\ \delta_3 \end{pmatrix} = \begin{pmatrix} -F_1 \\ -F_2 - f'(x_1)F_1 \\ \frac{-F_3 - f'(x_2)F_2 - f'(x_2)f'(x_1)F_1}{1 - f'(x_2)f'(x_1)f'(x_3)} \end{pmatrix}. \tag{14.10}$$

Finally we add $f'(x_3)$ times the third row to the first row and $f'(x_1)f'(x_3)$ times the third row to the second row. On the left hand side the matrix is now the unit matrix, on the right hand side we have the corrections to our initial guess for the cycle, i.e. we have gone through one step of the Newton iteration scheme.

When one sets up the Newton iteration on the computer it is not necessary to write the left hand side as a matrix. All one needs is a vector containing the $f'(x_i)$'s, a vector containing the n'th column, that is the cumulative product of the $f'(x_i)$'s and a vector containing the right hand side. After the iteration the vector containing the right hand side should be the correction to the initial guess.

14.1 page 276

14.4 d-dimensional mappings

(F. Christiansen)

Armed with symbolic dynamics informed initial guesses we can utilize the Newton-Raphson iteration in d-dimensions as well.

14.4.1 Newton's method for d-dimensional mappings

Newton's method for 1-dimensional mappings is easily extended to higher dimensions. In this case $f'(x_i)$ is a $[d \times d]$ matrix. $\frac{d}{dx}F(x)$ is then an $[nd \times nd]$ matrix. In each of the steps that we went through above we are then manipulating d rows of the left hand side matrix. (Remember that matrices do not commute - always multiply from the left.) In the inversion of the n'th element of the diagonal we are inverting a $[d \times d]$ matrix $(1 - \prod f'(x_i))$ which can be done if none of the eigenvalues of $\prod f'(x_i)$ equals 1, i.e. the cycle must not have any marginally stable directions.

Some d-dimensional mappings (such as the Hénon map (3.10)) can be written as 1-dimensional time delay mappings of the form

$$f(x_i) = f(x_{i-1}, x_{i-2}, \ldots, x_{i-d}). \tag{14.11}$$

In this case $\frac{d}{dx}F(x)$ is an $[n \times n]$ matrix as in the case of usual 1-dimensional maps but with non-zero matrix elements on d off-diagonals. In the elimination of these off-diagonal elements the last d columns of the matrix will become non-zero and in the final cleaning of the diagonal we will need to invert a $[d \times d]$ matrix. In this respect, nothing is gained numerically by looking at such maps as 1-dimensional time delay maps.

14.5 Flows

(F. Christiansen)

Further complications arise for flows due to the fact that for a periodic orbit the stability eigenvalue corresponding to the flow direction of necessity equals unity; the separation of any two points along a cycle remains unchanged after a completion of the cycle. More unit eigenvalues can arise if the flow satisfies conservation laws, such as the energy invariance for Hamiltonian systems. We now show how such problems are solved by increasing the number of fixed point conditions.

☞ sect. 4.5.3

14.5.1 Newton's method for flows

A flow is equivalent to a mapping in the sense that one can reduce the flow to a mapping on the Poincaré surface of section. An autonomous flow (2.5) is given as

$$\dot{x} = v(x), \tag{14.12}$$

The corresponding Jacobian matrix $\mathbf{J}$ (4.26) is obtained by integrating the linearized equation (4.28)

$$\dot{\mathbf{J}} = \mathbf{A}\mathbf{J}\,, \qquad A_{ij}(x) = \frac{\partial v_i(x)}{\partial x_j}$$

along the trajectory. The flow and the corresponding Jacobian matrix are integrated simultaneously, by the same numerical routine. Integrating an

initial condition on the Poincaré surface until a later crossing of the same and linearizing around the flow we can write

$$f(x') \approx f(x) + \mathbf{J}(x' - x). \tag{14.13}$$

Notice here, that, even though all of x', x and $f(x)$ are on the Poincaré surface, $f(x')$ is usually not. The reason for this is that $\mathbf{J}$ corresponds to a specific integration time and has no explicit relation to the arbitrary choice of Poincaré section. This will become important in the extended Newton's method described below.

To find a fixed point of the flow near a starting guess x we must solve the linearized equation

$$(1 - \mathbf{J})(x' - x) = -(x - f(x)) = -F(x) \tag{14.14}$$

where $f(x)$ corresponds to integrating from one intersection of the Poincaré surface to another and $\mathbf{J}$ is integrated accordingly. Here we run into problems with the direction along the flow, since this corresponds to a unit eigenvector of $\mathbf{J}$. The matrix $(1 - \mathbf{J})$ does therefore not have full rank. A related problem is that the solution x' of (14.14) is not guaranteed to be in the Poincaré surface of section. The two problems are solved simultaneously by adding a small vector along the flow plus an extra equation demanding that x be in the Poincaré surface. Let us for the sake of simplicity assume that the Poincaré surface is a (hyper)-plane, i.e. it is given by the linear equation

$$(x - x_0) \cdot a = 0, \tag{14.15}$$

where a is a vector normal to the Poincaré section and x_0 is any point in the Poincaré section. (14.14) then becomes

$$\begin{pmatrix} 1 - \mathbf{J} & v(x) \\ a & 0 \end{pmatrix} \begin{pmatrix} x' - x \\ \delta T \end{pmatrix} = \begin{pmatrix} -F(x) \\ 0 \end{pmatrix}. \tag{14.16}$$

The last row in this equation ensures that x will be in the surface of section, and the addition of $v(x)\delta T$, a small vector along the direction of the flow, ensures that such an x can be found at least if x is sufficiently close to a solution, i.e. to a fixed point of f.

To illustrate this little trick let us take a particularly simple example; consider a 3-d flow with the $(x, y, 0)$-plane as Poincaré section. Let all trajectories cross the Poincaré section perpendicularly, i.e. with $v = (0, 0, v_z)$,

which means that the marginally stable direction is also perpendicular to the Poincaré section. Furthermore, let the unstable direction be parallel to the x-axis and the stable direction be parallel to the y-axis. In this case the Newton setup looks as follows

$$\begin{pmatrix} 1-\Lambda & 0 & 0 & 0 \\ 0 & 1-\Lambda_s & 0 & 0 \\ 0 & 0 & 0 & v_z \\ 0 & 0 & 1 & 0 \end{pmatrix} \begin{pmatrix} \delta_x \\ \delta_y \\ \delta_z \\ \delta t \end{pmatrix} = \begin{pmatrix} -F_x \\ -F_y \\ -F_z \\ 0 \end{pmatrix}. \tag{14.17}$$

If you consider only the upper-left $[3\times 3]$ matrix (which is what we would have without the extra constraints that we have introduced) then this matrix is clearly not invertible and the equation does not have a unique solution. However, the full $[4\times 4]$ matrix is invertible, as $\det(\cdot) = v_z \det(1-\mathbf{J}_\perp)$, where $\mathbf{J}_\perp$ is the monodromy matrix for a surface of section transverse to the orbit, see for ex. (27.2).

For periodic orbits (14.16) generalizes in the same way as (14.7), but with n additional equations – one for each point on the Poincaré surface. The Newton setup looks like this

$$\left(\begin{array}{ccccc|ccc} 1 & & & & -J_n & v_1 & & \\ -J_1 & 1 & & & & & \ddots & \\ & \cdots & 1 & & & & & v_n \\ & & \cdots & 1 & & & & \\ & & & -J_{n-1} & 1 & & & \\ \hline & a & & & & 0 & & \\ & & \ddots & & & & \ddots & \\ & & & a & & & & 0 \end{array}\right) \begin{pmatrix} \delta_1 \\ \delta_2 \\ \cdot \\ \cdot \\ \delta_n \\ \delta t_1 \\ \cdot \\ \delta t_n \end{pmatrix} = \begin{pmatrix} -F_1 \\ -F_2 \\ \cdot \\ \cdot \\ -F_n \\ 0 \\ \cdot \\ 0 \end{pmatrix}.$$

Solving this equation resembles the corresponding task for maps. However, in the process we will need to invert an $[(d+1)n\times(d+1)n]$ matrix rather than a $[d\times d]$ matrix. The task changes with the length of the cycle.

This method can be extended to take care of the same kind of problems if other eigenvalues of the Jacobian matrix equal 1. This happens if the flow has an invariant of motion, the most obvious example being energy conservation in Hamiltonian systems. In this case we add an extra equation for x to be on the energy shell plus and extra variable corresponding to adding a small vector along the gradient of the Hamiltonian. We then have to solve

$$\begin{pmatrix} 1-\mathbf{J} & v(x) & \nabla H(x) \\ a & 0 & 0 \end{pmatrix} \begin{pmatrix} x'-x \\ \delta t \\ \delta E \end{pmatrix} = \begin{pmatrix} -(x-f(x)) \\ 0 \\ 0 \end{pmatrix} \tag{14.18}$$

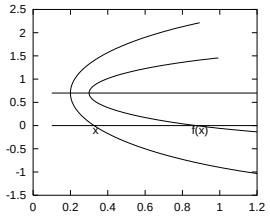

Figure 14.5: Illustration of the optimal Poincaré surface. The original surface $y=0$ yields a large distance $x-f(x)$ for the Newton iteration. A much better choice is $y=0.7$.

simultaneously with

$$H(x') - H(x) = 0. \tag{14.19}$$

This last equation is nonlinear. It is often best to treat this separately in the sense that we really solve this equation in each Newton step. This might mean putting in an additional Newton routine to solve the single step of (14.18) and (14.19) together. One might be tempted to linearize (14.19) and put it into (14.18) to do the two different Newton routines simultaneously, but this will not guarantee a solution on the energy shell. In fact, it may not even be possible to find any solution of the combined linearized equations, if the initial guess is not very good.

14.5.2 Newton's method with optimal surface of section

(F. Christiansen)

In some systems it might be hard to find a good starting guess for a fixed point, something that could happen if the topology and/or the symbolic dynamics of the flow is not well understood. By changing the Poincaré section one might get a better initial guess in the sense that x and $f(x)$ are closer together. In fig. 14.5 there is an illustration of this. The figure shows a Poincaré section, $y=0$, an initial guess x, the corresponding $f(x)$ and pieces of the trajectory near these two points.

If the Newton iteration does not converge for the initial guess x we might have to work very hard to find a better guess, particularly if this is in a high-dimensional system (high-dimensional might in this context mean a Hamiltonian system with 3 degrees of freedom.) But clearly we could easily have a much better guess by simply shifting the Poincaré section to

$y = 0.7$ where the distance $x - f(x)$ would be much smaller. Naturally, one cannot see by eye the best surface in higher dimensional systems. The way to proceed is as follows: We want to have a minimal distance between our initial guess x and the image of this $f(x)$. We therefore integrate the flow looking for a minimum in the distance $d(t) = |f^t(x) - x|$. $d(t)$ is now a minimum with respect to variations in $f^t(x)$, but not necessarily with respect to x. We therefore integrate x either forward or backward in time. Doing this we minimize d with respect to x, but now it is no longer minimal with respect to $f^t(x)$. We therefore repeat the steps, alternating between correcting x and $f^t(x)$. In most cases this process converges quite rapidly. The result is a trajectory for which the vector $(f(x) - x)$ connecting the two end points is perpendicular to the flow at both points. We can now choose to define a Poincaré surface of section as the hyper-plane that goes through x and is normal to the flow at x. In other words the surface of section is determined by

$$(x' - x) \cdot v(x) = 0. \tag{14.20}$$

Note that $f(x)$ lies on this surface. This surface of section is optimal in the sense that a close return on the surface is really a local minimum of the distance between x and $f^t(x)$. But more importantly, the part of the stability matrix that describes linearization perpendicular to the flow is exactly the stability of the flow in the surface of section when $f(x)$ is close to x. In this method, the Poincaré surface changes with each iteration of the Newton scheme. Should we later want to put the fixed point on a specific Poincaré surface it will only be a matter of moving along the trajectory.

☞ sect. 7.3.1

14.6 Stability of cycles for maps

No matter what method we had used to determine the unstable cycles, the theory to be developed here requires that their stability eigenvalues be evaluated as well. For maps a Jacobian matrix is easily evaluated by picking any cycle point as a starting point, running once around a prime cycle, and multiplying the individual cycle point stability matrices according to (4.31). For example, the Jacobian matrix $\mathbf{J}_p$ for a Hénon map (3.10) prime cycle p of length n_p is given by (4.32), and the Jacobian matrix $\mathbf{J}_p$ for a 2-dimensional billiard prime cycle p of length n_p follows from (5.22). As explained on page 72, evaluation of the Jacobian matrix for a flow will require an integration along the prime cycle.

☞ chapter 25

Commentary

Remark 14.1 Piece-wise linear maps. The Lozi map (3.12) is linear, and 100,000's of cycles can be easily computed by [2x2] matrix multiplication and inversion.

Résumé

There is no general computational algorithm that is guaranteed to find all solutions (up to a given period $T_{\max}$) to the periodic orbit condition

$$f^{t+T}(x) = f^t(x)\,, \qquad T > 0$$

for a general flow or mapping. Due to the exponential divergence of nearby trajectories in chaotic dynamical systems, direct solution of the periodic orbit condition can be numerically very unstable.

A prerequisite for a systematic and complete cycle search is a good (but hard to come by) understanding of the topology of the flow. Usually one starts by - possibly analytic - determination of the equilibria of the flow. Their locations, stabilities, stability eigenvectors and invariant manifolds offer skeletal information about the topology of the flow. Next step is numerical long-time evolution of "typical" trajectories of the dynamical system under investigation. Such numerical experiments build up the "natural measure", and reveal regions most frequently visited. The periodic orbit searches can then be initialized by taking nearly recurring orbit segments and deforming them into a closed orbits. With a sufficiently good initial guess the Newton-Raphson formula (14.16)

$$\begin{pmatrix} 1-\mathbf{J} & v(x) \\ a & 0 \end{pmatrix} \begin{pmatrix} \delta x \\ \delta T \end{pmatrix} = \begin{pmatrix} f(x)-x \\ 0 \end{pmatrix}$$

yields improved estimate $x' = x + \delta x, T' = T + \delta T$. Iteration then yields the period T and the location of a periodic point x_p in the Poincaré surface $(x_p - x_0) \cdot a = 0$, where a is a vector normal to the Poincaré section at x_0.

The problem one faces with high-dimensional flows is that their topology is hard to visualize, and that even with a decent starting guess for a point on a periodic orbit, methods like the Newton-Raphson method are likely to fail. Methods that start with initial guesses for a number of points along the cycle, such as the multipoint shooting method of sect. 14.3, are more robust.

The relaxation (or variational) methods take this strategy to its logical extreme, and start by a guess of not a few points along a periodic orbit, but a guess of the entire orbit. As these methods are intimately related to variational principles and path integrals, we postpone their introduction to chapter 25.

References

[14.1] D.W. Moore and E.A. Spiegel, "A thermally excited nonlinear oscillator", *Astrophys. J.*, **143**, 871 (1966).

[14.2] N.H. Baker, D.W. Moore and E.A. Spiegel, *Quar. J. Mech. and Appl. Math.* **24**, 391 (1971).

[14.3] E.A. Spiegel, *Chaos: a mixed metaphor for turbulence*, *Proc. Roy. Soc.* **A413**, 87 (1987).

[14.4] M. Baranger and K.T.R. Davies *Ann. Physics* **177**, 330 (1987).

[14.5] B.D. Mestel and I. Percival, *Physica D* **24**, 172 (1987); Q. Chen, J.D. Meiss and I. Percival, *Physica D* **29**, 143 (1987).

[14.6] find Helleman et all Fourier series methods

[14.7] J.M. Greene, *J. Math. Phys.* **20**, 1183 (1979)

[14.8] H.E. Nusse and J. Yorke, "A procedure for finding numerical trajectories on chaotic saddles" *Physica* **D 36**, 137 (1989).

[14.9] D.P. Lathrop and E.J. Kostelich, "Characterization of an experimental strange attractor by periodic orbits"

[14.10] T. E. Huston, K.T.R. Davies and M. Baranger *Chaos* **2**, 215 (1991).

[14.11] M. Brack, R. K. Bhaduri, J. Law and M. V. N. Murthy, *Phys. Rev. Lett.* **70**, 568 (1993).

[14.12] Z. Gills, C. Iwata, R. Roy, I.B. Scwartz and I. Triandaf, "Tracking Unstable Steady States: Extending the Stability Regime of a Multimode Laser System", *Phys. Rev. Lett.* **69**, 3169 (1992).